pISSN 1229-3008 eISSN 2287-6251
Progress in Superconductivity and Cryogenics
Vol.25, No.3, (2023), pp.22~27 https://doi.org/10.9714/psac.2023.25.3.022

Nonlocality effects of MgB_2 superconductor

Jeong Hun Yang, Jong Su You, Soo Kyung Lee, and Kyu Jeong Song*

Div. of Science Education and Institute of Sci. Education,
Jeonbuk National University, Jeonju, 54896 Korea

(Received 28 August 2023; revised or reviewed 27 September 2023; accepted 28 September 2023)

Abstract

Magnetic properties of MgB_2 superconducting powder were investigated. $M(H)$, the magnetic field H dependence of magnetization M, was measured and analyzed using a PPMS instrument. The MgB_2 superconducting powder showed high critical current density $J_c > \sim 10^7$ A/cm^2 and clean limit superconducting properties. The equilibrium magnetization M_{eq} properties of MgB_2 powders exhibiting various superconducting properties were studied. We find that the equilibrium magnetization $M_{eq}(H)$ properties of MgB_2 powders showing conventional BCS properties deviate from the predictions of the standard local-London theory at temperatures below T = 19 K and are in good agreement with the generalized nonlocal-London theory. Nonlocal-London analysis was used to determine and analyze the nonlocal parameters. The temperature dependence of the London penetration depth values $\lambda(T)$ was studied.

Keywords: MgB_2 powder, equilibrium magnetization, nonlocal-london theory, local-london theory, london penetration depth

1. INTRODUCTION

MgB_2 is a metallic two-component material and has a simple hexagonal crystal structure, but shows very diverse superconducting properties [1-3]. MgB_2 superconductors show conventional BCS superconducting properties similar to those of common metallic superconductors, but with a higher critical transition temperature ($T_c \sim 38$ K) compared to BCS low-temperature superconductors. They also show high critical current density ($J_c(0) > 10^7$ A/cm^2) due to strong coupling between grain boundaries, with a superconducting coherence length ($\xi(0) \sim 5$ nm) longer than the grain-boundary width ($d = 1 \sim 3$ nm) [2-5]. In particular, MgB_2 superconductors exhibit multi-band properties with weak scattering between bands, characterized by two-energy gaps: a cylindrical 2D-σ band ($\Delta_\sigma \sim 7.0$ meV) and an isotropic 3D-π band ($\Delta_\pi \sim 1.7$ meV) [6-12]. MgB_2 superconductors with two-bands and two-energy gaps exhibit a variety of superconducting properties and novel physical characteristics, and have been described by the anisotropic s-wave superconducting model of weakly coupled two-energy gaps [10]. In general, anisotropic superconducting properties are represented by a single anisotropic parameter, $\gamma = \xi_{ab}/\xi_c = \lambda_c/\lambda_{ab}$. However, the MgB_2 superconductor with weakly coupled two-energy gaps shows anisotropic parameter characteristics of $\gamma_{Hc2} \neq \gamma_\lambda$, where $\gamma_{Hc2} = H_{c2,ab} / H_{c2,c}$ is the upper-critical magnetic field anisotropic parameter and $\gamma_\lambda = \lambda_c/\lambda_{ab}$ is the London penetration depth anisotropic parameter. Here is $H_{c2,c} = \phi_0/2\pi\xi_{ab}^2$ and $H_{c2,ab} = \phi_0/2\pi\xi_{ab}\xi_c$. It is $\gamma_{Hc2} = \sim 6.0$ and $\gamma_\lambda = \sim 1.1$ near $T = \sim 0$ K, and exhibits a single anisotropic parameter $\gamma = \xi_{ab}/\xi_c = \lambda_c/\lambda_{ab}$ characteristic with $\gamma_{Hc2} = \gamma_\lambda = \sim 2.6$ near the critical transition temperature T_c [10]. Therefore, it can be predicted that the superconducting properties of MgB_2 in the temperature region near the critical transition temperature T_c and in the temperature region somewhat farther away from T_c will be somewhat different from each other.

On the other hand, the isotropic nature of the electrical conduction due to the long electron mean free path l and the upward curvature of the upper-critical magnetic field H_{c2} near T_c, similar to the nickel-borocarbide materials YNi_2B_2C and $LuNi_2B_2C$ superconductors, show that MgB_2 superconductors have clean limit superconducting properties [13]. The temperature dependence of γ_{Hc2} in the MgB_2 superconductor and the isotropic properties of γ_λ (~ 1.1) in the low temperature region far from T_c can also be explained by the clean limit superconductivity. The flux line lattice (FLL) structure change of nickel-borocarbide YNi_2B_2C superconductor with clean limit superconducting properties, i.e., from a triangular structure to a square structure, is well described by the generalized nonlocal-London theory, and the equilibrium magnetization M_{eq} properties of YNi_2B_2C superconductor in the low-temperature regime deviate somewhat from the conventional standard local-London theory predictions and are also well described by the generalized nonlocal-London theory [14].

Therefore, similar to the analysis of boron carbide YNi_2B_2C superconductor, this paper simultaneously performs a generalized nonlocal-London theory analysis based on the clean limit superconducting properties in the low temperature region far from T_c and a conventional standard local-London theory analysis based on the dirty limit superconducting properties in the high temperature region near T_c for the equilibrium magnetization M_{eq} values of MgB_2 superconducting powder samples. The

* Corresponding author: songkj@jbnu.ac.kr

magnetization $M(H)$ values were measured at 2 K temperature intervals from 5 K to 37 K using a physical property measurement system (PPMS) equipment, and the equilibrium magnetization M_{eq} values of the MgB_2 superconducting powder samples were analyzed from these $M(H)$ measurement data. The temperature dependence of the London penetration depth $\lambda(T)$ values obtained by applying the generalized nonlocal-London theory and the conventional local-London theory was analyzed, and the characteristics of the nonlocal parameters obtained by the generalized nonlocal-London theory analysis were also studied.

2. EXPERIMENTAL PROCEDURE

The MgB_2 powder sample used in this study is a commercially available powder sample purchased from Alfar Aesar company. As described in a previous paper [15], the purchased MgB_2 powder samples are pure MgB_2 powder samples with few impurity phases in XRD analysis. The mass of the MgB_2 powder sample used in the experiment is 0.23 g, and the theoretical density of the MgB_2 single crystal is 2.63 g/cm^3, so the superconductor volume of the MgB_2 powder sample used in the experiment is V_s = 0.087 cm^3. And in the analysis using a particle size analyzer, the average size of the MgB_2 powder sample is r = ~ 0.5 μm. The magnetic properties of the MgB_2 powder samples (powder in capsules) were measured by sweeping the magnetic field H at each temperature from 5 K to 37 K at 2 K intervals using a PPMS (Quantum Design (QD), USA). The magnetic field H applied during PPMS measurements was increased (or decreased) from 0 T to 9 T (or from 9 T to 0 T) to measure the magnetic field H intensity dependence $m(H)$ of the magnetic moment m at each temperature. The unit for magnetic moment m is [emu = G·cm^3]. The measured $m(H)$ data were divided by the superconductor volume of the sample, i.e., a value of V_s = 0.087 cm^3, to obtain the magnetic field H strength dependence $M(H)$ of the magnetization M for the MgB_2 powder sample. The unit of magnetization M is [G].

Meanwhile, the critical transition temperature, T_c, of the MgB_2 powder sample (powder in capsules) was determined by measuring and analyzing the temperature dependence of the magnetic moment, $m(T)$, under zero field cooling (ZFC) measurement conditions, i.e., decreasing the temperature, T = 5 K, without applying a magnetic field, then fixing it by applying a magnetic field, H = 10 G, and then increasing the temperature, T. And the magnetization $M(H)$ data was analyzed using the background magnetization $M(H)$ values measured at a temperature higher than the critical transition temperature T_c of the MgB_2 powder sample as correction values. The magnetic properties of the MgB_2 powder samples were analyzed by converting the measured magnetization M data into irreversible magnetization ΔM data. The irreversible magnetization $\Delta M = [M(H_{dec}) - M(H_{inc})]$ value, defined as the difference between the magnetization M values in the increasing and decreasing magnetic field regions, is the physical quantity associated with the critical current density J_c of the MgB_2 powder sample, and it can be used to predict the critical current density $J_c(H)$ through the Bean critical state model, i.e., the $J_c = 20\Delta M/r$ relation [16]. Where r is the mean grain radius, the average radius of the polycrystalline MgB_2 powder sample used in this study is r = ~ 0.5 μm. In addition, the magnetic properties of MgB_2 powder samples were analyzed by obtaining the magnetic field H dependence $M_{eq}(H)$ of the equilibrium magnetization M_{eq} by using the magnetic field H dependence $M(H)$ data of the magnetization M for MgB_2 powder samples. Here, the equilibrium magnetization M_{eq} value, defined as the average value of the magnetization M value in the increasing and decreasing magnetic field regions, was obtained by the formula $M_{eq} = [M(H_{dec}) + M(H_{inc})]/2$.

3. RESULTS AND DISCUSSION

A common measurement for investigating the magnetic properties of a superconducting sample using a PPMS magnetometer instrument is the $m(H)$ graph, which is the dependence of the magnetic field H on the magnetic moment m. For the MgB_2 superconducting powder sample, $m(H)$ graphs were measured at specific temperatures from 5 K to 37 K in 2 K intervals, respectively. That is, by measuring the change in $m(H)$ while increasing the magnetic field H intensity applied to the MgB_2 superconducting powder sample from 0 G to 9 T, and then measuring the change in $m(H)$ while decreasing the magnetic field H intensity from 9 T to 0 G, keeping each specific temperature in the 2 K interval constant, independent $m(H)$ graphs were obtained for each specific temperature in the 2 K interval. The magnetic moment $m(H)$ data were divided by the superconductor volume of the sample, V_s = 0.087 cm^3, to obtain $M(H)$ graphs, which are the magnetic field H dependence of the magnetization M for the MgB_2 superconducting powder sample. Fig. 1 shows $M(H)$ graphs, the dependence of magnetization M on magnetic field H, for a sample of MgB_2 superconducting powder at each specific temperature. As can be seen in Fig. 1, the $M(H)$ graphs are nearly top-to-bottom symmetric at M = 0 G. For most temperatures, the $M(H)$ data exhibit both irreversible ($\Delta M \neq 0$) and reversible ($\Delta M \approx 0$) magnetization properties.

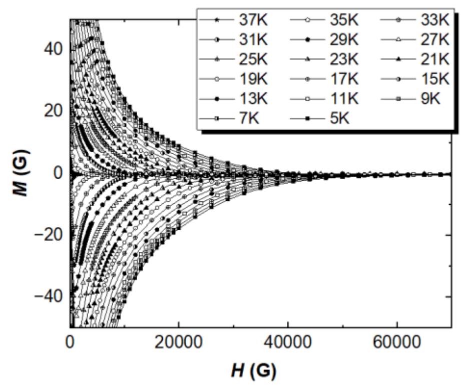

Fig. 1. The superconductive magnetization M versus magnetic field H of the pure MgB_2 powder, for temperatures from 5 K to 37 K in steps of 2 K.

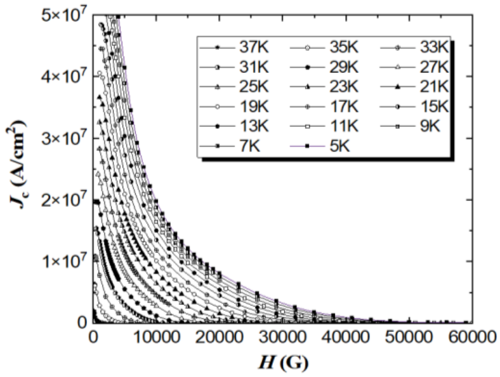

Fig. 2. The critical current density J_c versus magnetic field H of the pure MgB_2 powder, for temperatures from 5 K to 37 K in steps of 2 K.

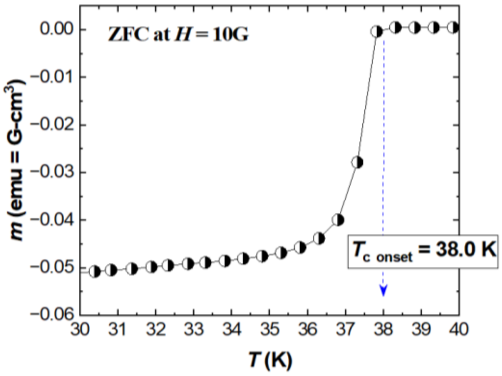

Fig. 3. The ZFC curve as the function of temperature T for the pure MgB_2 powder, with H = 10 G. The T_c was defined by the onset temperature.

Fig. 2 is a graph of $J_c(H)$, the dependence of the critical current density J_c on the magnetic field H, for the MgB_2 superconducting powder sample. The critical current density, J_c, is one of the typical physical quantities of superconducting materials in general. By applying the $M(H)$ data obtained from PPMS magnetization measurements to the Bean critical state model, the critical current density J_c values of MgB_2 superconducting powder samples can be predicted and determined. The Bean critical state model is represented by $J_c = 20\Delta M/r$ [16], where r is the mean grain radius, and ΔM is the irreversible magnetization, which is the difference between the magnetization $M(H_{inc})$ value in the magnetic field region where the magnetic field strength applied to the sample increases and the magnetization $M(H_{dec})$ value in the magnetic field region where the magnetic field strength decreases, i.e., $\Delta M = [M(H_{dec}) - M(H_{inc})]$. As shown in Fig. 2, it shows high critical current density ($J_c > \sim 10^7$ A/cm^2) characteristics due to strong coupling between grain boundaries. However, the critical current density J_c characteristic of MgB_2 superconducting powder samples without introducing artificial flux pinning defects is significantly degraded with increasing applied magnetic field H strength, showing $J_c \sim 0$ in the region of $H > 4$ T and above.

Fig. 3 is a graph of $m(T)$ obtained by measuring the dependence of the magnetic moment m on temperature T under ZFC (zero field cooling) conditions. First, after lowering to a temperature T = 5 K below the critical transition temperature T_c with no magnetic field H applied, and then a magnetic field strength of H = 10 G is applied at temperature T = 5 K. Under these ZFC conditions, keeping H = 10 G, the magnetic moment m is measured with slowly increasing the temperature T from 5 K to 50 K, that is, a graph of $m(T)$ is obtained. As shown in Fig. 3, the temperature at which the diamagnetic or Meissner effect characteristics ($m(T) < 0$) start in the $m(T)$ graph is determined as the critical transition temperature T_c, and the T_c of the MgB_2 superconducting powder sample is 38.0 K.

As described in the introduction, MgB_2 superconductors exhibit conventional BCS electron-phonon mechanism superconducting properties [17], but due to the nature of the two bands and two energy gaps, they exhibit a variety of novel superconducting and physical properties [2-12]. The temperature-dependent $\lambda(T)$ characteristics of London penetration depth λ are related to the size of the energy gaps: in the high temperature region near the critical transition temperature T_c, the $\lambda(T)$ is strongly influenced by the wide energy gap of the 2D-σ band ($\Delta_\sigma \sim 7.0$ meV), while in the low temperature region, $T \ll T_c$, the $\lambda(T)$ is strongly influenced by the narrow energy gap of the 3D-π band ($\Delta_\pi \sim 1.7$ meV) [8-11]. In addition, one of the interesting properties of MgB_2 superconductors is the change in their anisotropic superconducting properties. The two bands and two energy gaps characterize anisotropic superconductivity as $\gamma_{Hc2} \neq \gamma_\lambda$ in the low temperature region, which is $T \ll T_c$, and as $\gamma_{Hc2} = \gamma_\lambda$ in the high temperature region near T_c, that is, a single anisotropic parameter $\gamma = \xi_{ab}/\xi_c = \lambda_c/\lambda_{ab}$ characteristic [10]. Therefore, we can predict that there are different superconducting mechanisms in the two temperature regions, one at $T \ll T_c$ and the other near T_c.

It can be predicted that MgB_2 superconductor is a clean limit superconductor because of its long electron mean free path l and upward curvature characteristic in the upper critical magnetic field H_{c2}. If the superconductivity of clean-limit MgB_2 is truly nonlocal, then its equilibrium mixed-state (vortex-state) properties, like those of borocarbide clean-limit YNi_2B_2C superconductors, are very difficult to explain with the conventional local-London theory and must be explained with a generalized nonlocal-London theory [14]. Therefore, it should be shown that the equilibrium magnetization M_{eq} properties of MgB_2 superconducting powder samples deviate from the predictions of the local-London theory and are in good agreement with the predictions of the generalized nonlocal-London theory. Therefore, to obtain $M_{eq}(H)$, the magnetic field H dependence of the equilibrium magnetization M_{eq} for the MgB_2 powder sample, we used the $M(H)$ data, the magnetic field H dependence of the magnetization M shown in Fig. 1. Here, the equilibrium magnetization M_{eq} value is defined as the average value of the magnetization M values in the increasing and decreasing magnetic field regions, and is obtained using the $M_{eq} = [M(H_{dec})+M(H_{inc})]/2$ equation. Fig. 4 shows the semi-logarithmic relationship between the

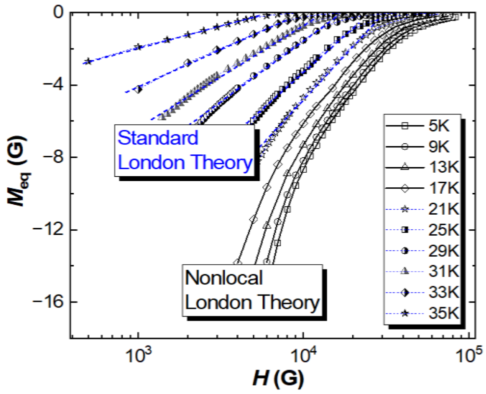

Fig. 4. A semilogarithmic plot of equilibrium magnetization M_{eq} versus magnetic field H of the pure MgB_2 powder, for temperatures from 5 K to 35 K.

equilibrium magnetization, M_{eq}, and the magnetic field, H, for temperatures from T = 5 K to 35 K. As can be seen in Fig. 4, there is a clear distinction between non-linear graphs for temperatures below T = 19 K and linear graphs for temperatures above T = 21 K. In general, linear graphs above temperature T = 21 K are well explained by the standard local-London theory, and nonlinear graphs below temperature T = 19 K can be explained relatively well by the generalized nonlocal-London theory.

According to standard local-London theory, in a magnetic field region of $H_{c1} \ll H \ll H_{c2}$, the relation between the equilibrium magnetization M_{eq} and the magnetic field H is expressed as $M_{eq} = - M_0 \ln(\eta H_{c2}/H)$ [18]. Where M_0 is the $M_0 = \phi_0/32\pi^2\lambda_{ab}^2$, $H_{c1} = \phi_0 \ln(\lambda_{ab}/\xi)/4\pi\lambda_{ab}^2$ is the lower-critical magnetic field, $H_{c2} = \phi_0/2\pi\xi^2$ is the upper-critical magnetic field, η is a constant of base unit size, λ_{ab}^2 is the London penetration depth, and ξ is the Ginzburg-Landau coherence length. Thus, as shown in Fig. 4, the linear graphs above temperature T = 21 K are well described by the standard local-London theory of a logarithmic magnetic field (ln$H$) dependence on the equilibrium magnetization M_{eq}, i.e., a proportional relationship of $M_{eq} \propto \ln H$. At temperatures above T = 21 K in Fig. 4, the slope of the linear graph is equal to the M_0 value. Therefore, we can obtain the slope values at each temperature above T = 21 K in Fig. 4, and apply these slope values to the $M_0 = \phi_0/32\pi^2\lambda_{ab}^2$ equation to predict the London penetration depth λ_{ab}^2 at each temperature. We will return to this discussion when we describe Fig. 6.

On the other hand, the properties of nonlinear graphs at temperatures below T = 19 K in Fig. 4 cannot be explained by the proportional relationship of $M_{eq} \propto \ln H$, the standard local-London theory. The generalized nonlocal-London theory of Kogan-Gurevich is obtained by introducing a nonlocality-radius ρ that depends on the mean free path l, and applying a new concept of $H_0 = \phi_0/2\pi^2 3^{1/2}\rho^2$ magnetic field instead of $H_{c2} = \phi_0/2\pi\xi^2$ for the equilibrium magnetization M_{eq} [19-20]. Here, the nonlocality radius ρ slowly decreases with increasing temperature, which is the opposite property of the Ginzburg-Landau coherence length ξ. According to the generalized nonlocal-London theory applying these length ρ and magnetic field H_0 scales, the relationship between the equilibrium magnetization M_{eq} and the magnetic field H in the $H_{c1} \ll H \ll H_{c2}$ magnetic field region is expressed as $M_{eq} = -M_0[\ln(H_0/H + 1) - H_0/(H_0+H) + \zeta]$ [19-20]. Here $M_0 = \phi_0/32\pi^2\lambda_{ab}^2$ is the same as in the local-London theory, the new magnetic field scale magnetic field H_0 is $H_0 = \phi_0/2\pi^2 3^{1/2}\rho^2$, and the dimensionless quantity ζ is $\zeta(T) = \eta_1 - \ln(H_0/\eta_2 H_{c2} + 1)$ represented by the basic unit size constants η_1 and η_2. From Fig. 4, it can be seen that in the temperature region below T = 19 K, the nonlinear graphs are in good agreement with the generalized nonlocal-London theory, and as the temperature increases, the degree of curvature of the nonlinear graphs in the $H_{c1} \ll H \ll H_{c2}$ magnetic field region gradually decreases and becomes increasingly linear, and near the critical transition temperature T_c, the graphs are almost completely linear. It can be seen that the clean limit MgB_2 superconducting properties exhibit nonlocal superconducting properties in the temperature region of $T \ll T_c$, and then the nonlocal superconducting properties

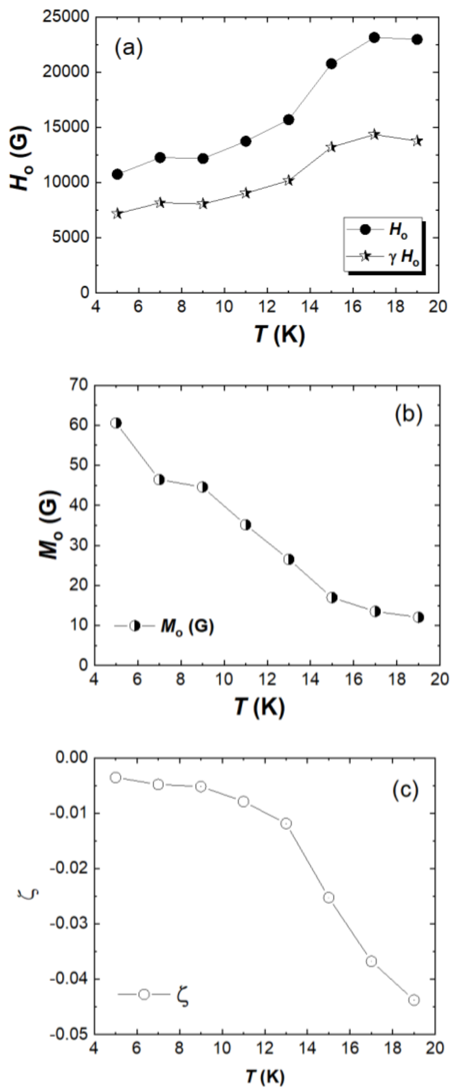

Fig. 5. Parameters from nonlocal London analysis versus temperatures for the pure MgB_2 powder: (a) the field scale H_0 and product γH_0, (b) the magnetization M_0, and (c) dimensionless quantity ζ.

gradually disappear with increasing temperature, and change to fully local superconducting properties near T_c in the high temperature region.

In Fig. 4, the nonlinear graphs in the temperature region below T = 19 K can be applied to the generalized nonlocal-London theoretical relation to obtain three nonlocal parameters: H_0, M_0, and ζ. This means that the values of the parameters H_0, M_0, and ζ can be determined for each temperature by substituting the nonlinear graph data for each temperature into the generalized nonlocal-London theoretical expression and fitting those. Fig. 5 shows the temperature dependence of the nonlocal parameters, namely $H_0(T)$, $M_0(T)$, and $\zeta(T)$ graphs. When T = 5 K from the $H_0 = \phi_0/2\pi^2 3^{1/2}\rho^2$ relational expression, nonlocality-radius ρ is calculated to be $\rho \approx 7.40 \times 10^{-8}$ m. Since the nonlocal-radius ρ depends on the mean free path l, we can predict the long mean free path l of the MgB_2 powder sample, and thus predict that the MgB_2 powder sample has clean limit superconducting properties.

As shown in Fig. 5(a), we can see that the $H_0(T)$ value increases as the temperature increases. The temperature dependence of the calculated γH_0 value is shown in Fig. 5(a) by selecting the $\gamma(T)$ value of the clean limit condition which is $\xi/l \approx 0$, from the $\gamma(T)$ values calculated by V. G. Kogan [20]. For the borocarbide clean limit YNi_2B_2C superconductor, the γH_0 value is constant with increasing temperature, as predicted by the generalized nonlocal-London theory [14], but for our clean limit MgB_2 powder sample, the γH_0 value increases rather weakly with increasing temperature. These results are considered to be due to irreversible characteristics in a wide magnetic field region, as shown in the magnetization $M(H)$ graph of the clean limit MgB_2 powder sample. In general, the generalized nonlocal-London theory can be applied to clean limit superconductors that exhibit a large region of reversibility in the magnetization $M(H)$ graph, and their experimental results are well explained by nonlocality. On the other hand, similar to the nonlocality results of borocarbide YNi_2B_2C superconductors and HTS superconductors [14], it can be seen that the $M_0(T)$ and $\zeta(T)$ values gradually decrease with increasing temperature, as shown in Figs. 5(b) and 5(c). By applying and analyzing the generalized nonlocal-London theory, we can predict the London penetration depth λ_{ab}^2 for each temperature from the $M_0 = \phi_0/32\pi^2\lambda_{ab}^2$ values obtained in the lower temperature regime below T = 19 K. This will be discussed in conjunction with the London penetration depth λ_{ab}^2 for each temperature in the higher temperature region above T = 21 K obtained by applying standard local-London theory when explaining Fig. 6.

Fig. 6 shows the temperature dependence of $1/\lambda^2$ for a clean limit MgB_2 superconducting powder sample. As explained earlier and shown in Fig. 6, the $1/\lambda^2$ values for the temperature region below T = 19 K are obtained by applying the generalized nonlocal-London theory, while the $1/\lambda^2$ values for the temperature region above T = 21 K are obtained by applying the standard local-London theory. Furthermore, as shown in the inset of Fig. 6, it can be seen that the temperature dependence of the $1/\lambda^2$ values obtained

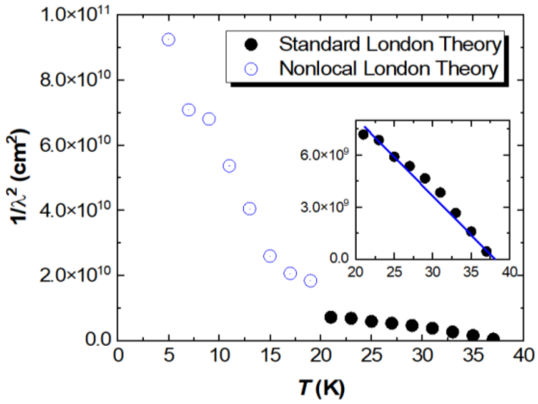

Fig. 6. The temperature dependence of London penetration depth λ for the pure MgB_2 powder. In inset, the straight line shows Ginzburg-Landau behavior near T_c, for data obtained from standard London analysis.

by applying the standard local-London theory near the criti cal transition temperature T_c is almost linear, as predicted by the Ginzburg-Landau theory [21-23], which predicts tha t the MgB_2 powder sample exhibits clean limit BCS conve ntional superconducting properties.

4. SUMMARY

In the low temperature region away from the critical transition temperature T_c, i.e., at temperatures below T = 19 K, where $T \ll T_c$, the equilibrium magnetization M_{eq} properties of the clean limit MgB_2 superconducting powder sample deviated from the predictions of the standard local-London theory, but agreed with the predictions of the generalized nonlocal-London theory with some accuracy. However, at temperatures above T = 21 K, the equilibrium magnetization M_{eq} properties of the clean limit MgB_2 superconducting powder sample were in exact agreement with the predictions of the conventional standard local-London theory. The nonlocal-London effect, which appears at temperatures below T = 19 K, gradually disappears at temperatures above T = 21 K. In the temperature region near the critical transition temperature T_c, the results are fully consistent with the standard local-London theory. Meanwhile, the London penetration depth λ_{ab}^2 of the clean limit MgB_2 superconducting powder sample was obtained by applying the nonlocal-London theory at temperatures below T = 19 K and the local-London theory at temperatures above T = 21 K, respectively. The linear temperature dependence of $1/\lambda^2$ obtained by applying the local-London theory in the temperature region near the critical transition temperature T_c is similar to the results predicted by the Ginzburg-Landau theory.

ACKNOWLEDGMENT

This work was supported by a grant from the Basic Science Research Program, administered through the

National Research Foundation of Korea (NRF) and funded by the Ministry of Education (NRF-2021R1A2C1094771).

REFERENCES

[1] J. Nagamatsu, N. Nagagawa, T. Muranaka, Y. Zenitani and J. Akimitsu, "Superconductivity at 39 K in magnesium diboride," *Nature*, vol. 401, pp. 63, 2001.

[2] C. Buzea and T. Yamashita, "Review of superconducting properties of MgB_2," *Supercond. Sci. Technol.*, vol. 14, pp. R115-R150, 2001, and references therein.

[3] "The second special issu of Physica C on MgB_2" edited by Setsuko Tajima, *Physica C*, vol. 456, pp. 1, 2007, and references therein.

[4] D. K. Finnemore, J. E. Ostenson, S. L. Bud'ko, G. Lapertot and P. C. Canfield, "Thermodynamic and transport properties of superconducting $Mg^{10}B_2$," *Phys. Rev. Lett.*, vol. 86, pp. 2420, 2001.

[5] D. C. Larbalestier, L. D. Cooley, M. O. Rikel, A. A. Polyanskii, J. Y. Jiang, et al., "Strongly linked current flow in polycrystalline forms of the superconductor MgB_2," *Nature*, vol. 410, pp. 186-189, 2001.

[6] H. J. Choi, D. Roundy, H. Sun, M. L. Cohen and S. G. Louie, "The origin of the anomalous superconducting properties of MgB_2," *Nature*, vol. 418, pp. 758-760, 2002.

[7] S. Souma, Y. Machida, T. Sato, T. Takahashi, H. Matsui, et al., "The origin of multiple superconducting gaps in MgB_2," *Nature*, vol. 423, pp. 65-67, 2003.

[8] M. S. Kim, J. A. Skinta, T. R. Lemberger, W. N. Kang, H.-J. Kim, E.-M. Choi and S.-I. Lee, "Reflection of a two-gap nature in penetration-depth measurement of MgB_2 film," *Phys. Rev. B*, vol. 66, pp. 064511, 2002.

[9] F. Manzano, A. Carrington, N. E. Hussey, S. Lee, A. Yamamoto and S. Tajima, "Exponential temperature dependence of the penetration depth in single crystal MgB_2," *Phys. Rev. Lett.*, vol. 88, 047002, 2002.

[10] V. G. Kogan and S. L. Bud'ko, "Anisotropy parameters of superconducting MgB_2," *Physica C*, vol. 385, pp. 131-142, 2003, and references therein.

[11] Byeongwon Kang, Heon-Jung Kim, Min-Seok Park, Kyung-Hee Kim and Sung-Ik Lee, "Reversible magnetization of MgB_2 single crystals with a two-gap nature," *Phys. Rev. B*, vol. 69, pp. 144514, 2004.

[12] Heon-Jung Kim, Byeongwon Kang, Min-Seok Park, Kyung-Hee Kim, Hyun Sook Lee and Sung-Ik Lee, "Reversible magnetization measurement of the anisotropy of the London penetration depth in MgB_2 single crystals," *Phys. Rev. B*, vol. 69, pp. 184514, 2004.

[13] G. Fuchs, K.-H. Muller, A. Handstein, K. Nemkov, V. N. Narozhnyi, D. Eckert, M. Wolf and L. Schultz, "Upper critical field and irreversibility line in superconducting MgB_2," *Solid State Communications*, vol. 118, pp. 497-501, 2001.

[14] K. J. Song, J. R. Thompson, M. Yethiraj, D. K. Christen, C. V. Tomy and D. Mck. Paul, "Nonlocal current-field relation and the vortex-state magnetic properties of YNi_2B_2C," *Phys. Rev. B*, vol. 59, pp. R6620-R6623, 1999.

[15] K. J. Song, J. C. Lim, S. Kang, R. K. Ko, K. C. Chung, S. Yoon and C. Park, "The effect of diluted water treatments on the superconducting properties of MgB_2," *IEEE Trans. on Appl. Supercond.*, vol. 23, pp. 7100304, 2013.

[16] C. P. Bean, "Magnetization of high-field superconductors," *Rev. Mod. Phys.*, vol. 36, pp. 31-36, 1964.

[17] S. L. Bud'ko, G. Lapertot, C. Petrovio, C. E. Cunningham, N. Anderson and P. C. Canfield, "Boron isotope effect in superconducting MgB_2," *Phys. Rev. Lett.*, vol. 86, pp. 1877-1880, 2001.

[18] V. G. Kogan, M. M. Fang and Sreeparna Mitra, "Reversible magnetization of high-T_c materials in intermediated fields," *Phys. Rev. B*, vol. 38, pp. 11958, 1988.

[19] V. G. Kogan, M. Bullock, B. Harmon, P. Miranovic, Lj. Dobrosavljevic-Grujic, P. L. Gammel and D. J. Bishop, "Vortex lattice transitions in borocarbides," *Phys. Rev. B*, vol. 55, R8693, 1997.

[20] V. G. Kogan, A. Gurevich, J. H. Cho, D. C. Johnston, Ming Xu, J. R. Thompson and A. Martynovich, "Nonlocal electrodynamics and low-temperature magnetization of clean high-κ superconductors," *Phys. Rev. B*, vol. 54, pp. 12386, 1996.

[21] P. De Gennes, *Superconductivity of Metals and Alloys*, Addison-Wesley, New York, 1989.

[22] M. Tinkham, *Introduction to superconductivity*, McGraw-Hill, New York, 1996.

[23] A. A. Abrikosov, *Fundamentals of the theory of metals*, North-Holland, New York, 1988.